



## ■ CARTILAGE

# Suramin enhances chondrogenic properties by regulating the p67<sup>phox</sup>/PI3K/AKT/SOX9 signalling pathway

Z-M. Liu,  
P-C. Shen,  
C-C. Lu,  
S-H. Chou,  
Y-C. Tien

From Kaohsiung  
Medical University,  
Kaohsiung, Taiwan

## Aims

Autologous chondrocyte implantation (ACI) is a promising treatment for articular cartilage degeneration and injury; however, it requires a large number of human hyaline chondrocytes, which often undergo dedifferentiation during *in vitro* expansion. This study aimed to investigate the effect of suramin on chondrocyte differentiation and its underlying mechanism.

## Methods

Porcine chondrocytes were treated with vehicle or various doses of suramin. The expression of collagen, type II, alpha 1 (COL2A1), aggrecan (ACAN); COL1A1; COL10A1; SRY-box transcription factor 9 (SOX9); nicotinamide adenine dinucleotide phosphate (NADPH) oxidase (NOX); interleukin (IL)-1 $\beta$ ; tumour necrosis factor alpha (TNF $\alpha$ ); IL-8; and matrix metalloproteinase 13 (MMP-13) in chondrocytes at both messenger RNA (mRNA) and protein levels was determined by quantitative reverse transcriptase polymerase chain reaction (qRT-PCR) and western blot. In addition, the supplementation of suramin to redifferentiation medium for the culture of expanded chondrocytes in 3D pellets was evaluated. Glycosaminoglycan (GAG) and collagen production were evaluated by biochemical analyses and immunofluorescence, as well as by immunohistochemistry. The expression of reactive oxygen species (ROS) and NOX activity were assessed by luciferase reporter gene assay, immunofluorescence analysis, and flow cytometry. Mutagenesis analysis, Alcian blue staining, reverse transcriptase polymerase chain reaction (RT-PCR), and western blot assay were used to determine whether p67<sup>phox</sup> was involved in suramin-enhanced chondrocyte phenotype maintenance.

## Results

Suramin enhanced the COL2A1 and ACAN expression and lowered COL1A1 synthesis. Also, in 3D pellet culture GAG and COL2A1 production was significantly higher in pellets consisting of chondrocytes expanded with suramin compared to controls. Surprisingly, suramin also increased ROS generation, which is largely caused by enhanced NOX (p67<sup>phox</sup>) activity and membrane translocation. Overexpression of p67<sup>phox</sup> but not p67<sup>phox</sup>AD (deleting amino acid (a.a) 199 to 212) mutant, which does not support ROS production in chondrocytes, significantly enhanced chondrocyte phenotype maintenance, SOX9 expression, and AKT (S473) phosphorylation. Knockdown of p67<sup>phox</sup> with its specific short hairpin (sh) RNA (shRNA) abolished the suramin-induced effects. Moreover, when these cells were treated with the phosphoinositide 3-kinase/protein kinase B (PI3K/AKT) inhibitor LY294002 or shRNA of AKT1, p67<sup>phox</sup>-induced COL2A1 and ACAN expression was significantly inhibited.

## Conclusion

Suramin could redifferentiate dedifferentiated chondrocytes dependent on p67<sup>phox</sup> activation, which is mediated by the PI3K/AKT/SOX9 signalling pathway.

**Cite this article:** *Bone Joint Res* 2022;11(10):723–738.

**Keywords:** Suramin, Reactive oxygen species, NADPH oxidase, p67<sup>phox</sup>, Chondrocyte redifferentiation

Correspondence should be sent to  
Yin-Chun Tien; email:  
chondrocyte@yahoo.com

doi: 10.1302/2046-3758.1110.BJR-  
2022-0013.R2

*Bone Joint Res* 2022;11(10):723–  
738.

## Article focus

- This study aimed to investigate the effects of suramin on chondrocyte differentiation maintenance, and its underlying molecular mechanism.

## Key messages

- Suramin treatment induced the upregulation of the collagen, type II, alpha 1 (COL2A1); aggrecan (ACAN); and SRY-box transcription factor 9 (SOX9), and downregulation of COL1A1, contributing to the differentiation of chondrocytes.
- However, suramin treatment enhanced the generation of reactive oxygen species (ROS) which is largely caused by nicotinamide adenine dinucleotide phosphate (NADPH) oxidase (NOX2)/p67<sup>phox</sup>.
- The redifferentiation of dedifferentiated chondrocytes under in vitro expansion was associated with an increase in expression of p67<sup>phox</sup> in chondrocytes.

## Strengths and limitations

- Our study may provide a new therapeutic option for improving chondrocyte phenotype maintenance.
- The effects of suramin on chondrocyte phenotype maintenance were not tested in an in vivo animal model.

## Introduction

It is known that articular cartilage defects have difficulty healing spontaneously due to limited tissue vascularization and a shortage of resident progenitor stem cells.<sup>1</sup> Treatment strategies that aim to reconstruct articular tissue have been developed, such as autologous chondrocyte implantation (ACI), microfracture, and mosaicplasty.<sup>2</sup> ACI for cartilage regeneration requires an adequate quantity of chondrocytes. Thus, in vitro monolayer expansion is required, and has been extensively adopted in order to apply this treatment. However, during in vitro expansion chondrocytes lose their phenotype, senescence, and dedifferentiate with serial passages, causing a substantial barrier to obtaining enough hyaline chondrocytes for transplantation. Furthermore, a previous study has demonstrated a “dedifferentiated-like” phenotype that might lead to chondrocyte degeneration.<sup>3</sup> However, little is known about the mechanisms underlying dedifferentiation.

Senescence and dedifferentiation of chondrocytes during monolayer culture are accompanied by decreased expression of matrix proteins such as type II collagen (COL II) and aggrecan (ACAN), which are regulated by several growth and transcription factors such as insulin-like growth factor 1 (IGF-1), transforming growth factor- $\beta$  (TGF- $\beta$ ), bone morphogenetic protein 2 (BMP-2), and SRY-box transcription factor 9 (SOX9).<sup>4,5</sup> Conversely, the levels of type I collagen (COL1A), matrix metalloproteinase 1 (MMP1), MMP3, MMP13, type X collagen (Col X), and interleukin-1 $\beta$  (IL-1 $\beta$ ) are upregulated during the inhibition of the normal molecular function of chondrocytes.<sup>6,7</sup> In addition, histone deacetylases (HDACs) (epigenetic factors), epigenetically regulate chromatin remodelling,

and transcription factor activity have been implicated in mediating chondrocyte phenotype. For example, HDAC activity in articular chondrocytes (ACs) decreases during dedifferentiation induced by serial monolayer culture, and another report reveals that overexpression of HDAC4 in proliferating chondrocytes suppresses hypertrophy and ossification of developing bones.<sup>8</sup> Further, overexpression of microRNA (miR)-486 markedly downregulates the expression of sirtuin 6 (SIRT6) (class III HDACs), and leads to upregulating the expression of ADAMTS4 and MMP-13 and downregulating the expression of COL2A1 and ACAN, consequently leading to catabolic phenotype in human osteochondroma cell line SW1353.<sup>9</sup>

Multiple studies have demonstrated that the intracellular redox status of chondrocytes plays an important role in the regulation of chondrocyte differentiation and chondrogenesis. In general, reactive oxygen species (ROS) and reactive nitrogen species (RNS) are the main factors that affect intracellular redox status. When redox homeostasis is disrupted, overproduction of ROS leads to oxidative stress, which has long been regarded as a critical factor in the induction of chondrocyte senescence and apoptosis in osteoarthritis (OA).<sup>10,11</sup> Many recent studies have revealed that the physiological levels of ROS act as an important signalling messenger in chondrocyte differentiation and metabolism.<sup>12,13</sup> The particular role of redox levels in articular cartilage remains unclear, and the mechanisms behind ROS signalling pathways has yet to be fully investigated.

The major ROS produced by chondrocytes are superoxide (O<sub>2</sub><sup>-</sup>), hydrogen peroxide (H<sub>2</sub>O<sub>2</sub>), nitric oxide (NO), and peroxynitrite, a reaction product of O<sub>2</sub><sup>-</sup> and NO.<sup>14</sup> The nicotinamide adenine dinucleotide phosphate (NADPH) oxidase (NOX) enzyme family is the main enzymatic source of O<sub>2</sub><sup>-</sup> and H<sub>2</sub>O<sub>2</sub>. NOX isoforms include NOX1, NOX2, NOX3, NOX4, NOX5, dual oxidase 1 (DUOX1), and DUOX2.<sup>15</sup> Chondrocytes express NOX2 and NOX4. Of these combinations, the NOX2 complex is composed of two membrane-bound subunits (p22<sup>phox</sup> and gp91<sup>phox</sup>), various cytosolic proteins (p40<sup>phox</sup>, p47<sup>phox</sup>, and p67<sup>phox</sup>), and Rac1 GTPase. In unstimulated conditions, the complex is latent, with unassembled subunits located in the cytosol and plasma membranes. Upon stimulation, the cytosolic components p47<sup>phox</sup>, p67<sup>phox</sup>, p40<sup>phox</sup>, and Rac2 translocate to the plasma membrane and associate with p22<sup>phox</sup>. Previous studies have shown that ROS produced by NOX2 and NOX4 are involved in chondrocyte differentiation.<sup>16,17</sup> NOX4 is required early in cartilage differentiation, and ROS produced by NOX1 may play a major role in chondrocyte terminal differentiation.<sup>13</sup> In addition, NOX2 has also been demonstrated in chondrocyte cell death mediated by IL-1 $\beta$ <sup>18</sup> and NOX4 in IL-1 $\beta$  stimulation of extracellular matrix (ECM) destruction enzyme expression.<sup>17</sup> Hence, ROS derived from NOX2 can be said to play a role in promoting ECM production, whereas NOX-2 does not seem to reduce ECM production.<sup>12</sup> These results proved that early chondrocyte differentiation and hypertrophy were stimulated by the expression of NOX and were dependent on the cellular context.

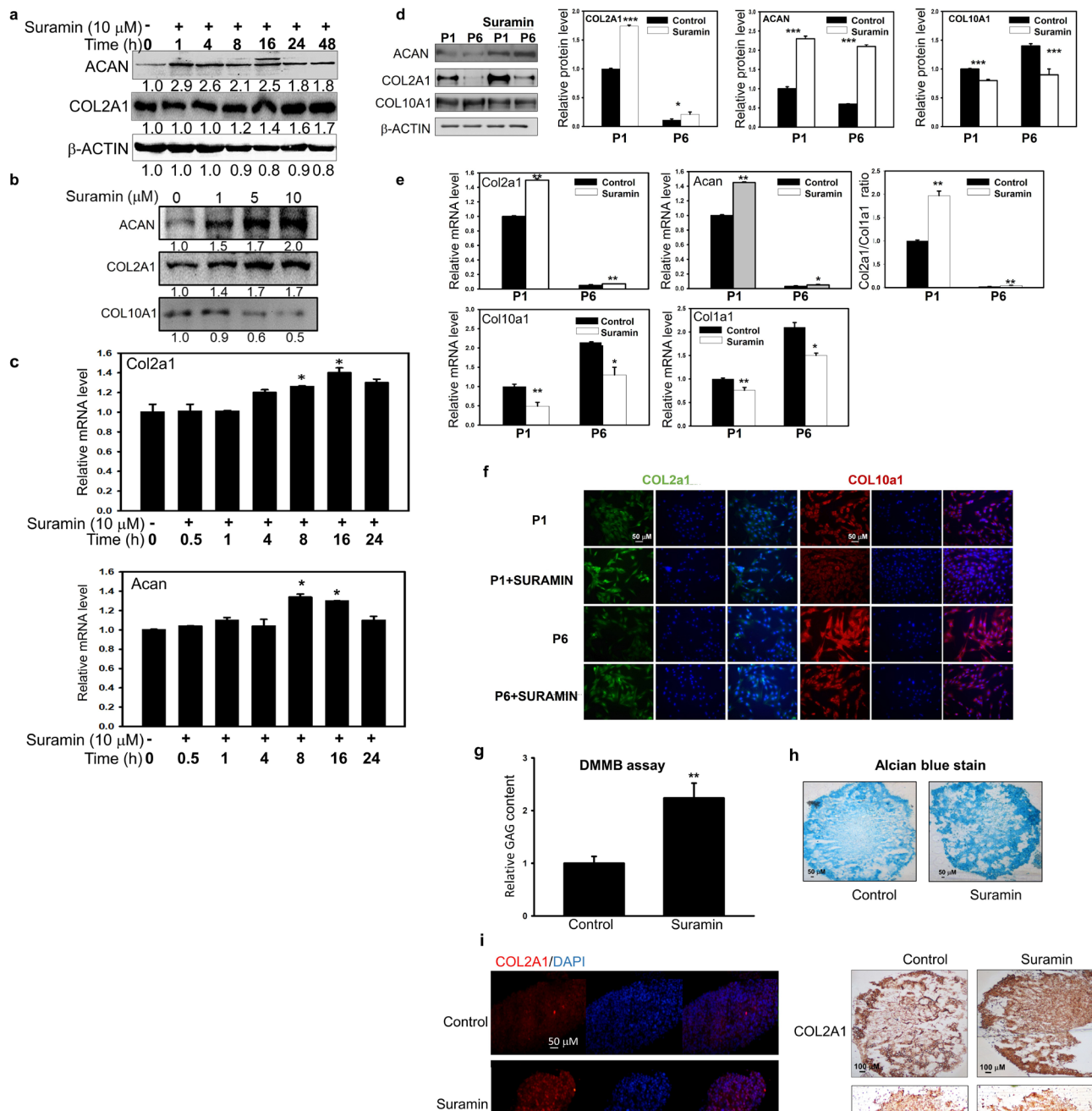


Fig. 1

Effect of suramin on chondrogenic and hypertrophic marker gene expression in chondrocytes. The P3 passage of chondrocytes were treated: a) with or without 10  $\mu$ M suramin for various timepoints; or b) with different amounts of suramin (0 to 10  $\mu$ M) for one day, and the protein expressions of collagen, type II, alpha 1 (COL2A1), COL10A1, and aggrecan (ACAN) were analyzed by western blot, with  $\beta$ -actin as the loading control. c) The chondrocytes were incubated with or without 10  $\mu$ M suramin for 0.5 hours to 24 hours, and the messenger RNA (mRNA) levels of *Col2a1* and *Acan* were detected by quantitative reverse transcriptase polymerase chain reaction (qRT-PCR). d) Early (P1) or later passage (P6) of chondrocytes were treated with or without suramin, and the protein expressions of COL2A1, COL10A1, and ACAN were analyzed by western blot. e) Relative mRNA levels in chondrocytes treated with or without suramin were tested for cartilage-specific markers such as *Col2a1*, *Col10a1*, and *Acan*, as well as *Col1* (dedifferentiation marker) using qRT-PCR ( $n = 3$ ). Values were normalized to glyceraldehyde 3-phosphate dehydrogenase levels. Data are shown as mean (standard deviation (SD)); \* $p < 0.05$ , \*\* $p < 0.01$ , and \*\*\* $p < 0.001$ . f) Representative immunofluorescence images of COL2A1 (green) and COL10A1 (red). Nuclei were stained with 4',6-diamidino-2-phenylindole (DAPI) (blue). g) Chondrocyte pellets were treated with or without suramin for 28 days and dimethylmethylene blue (DMMB) assay determining total sulphated glycosaminoglycan content normalized to DNA content; \*\* $p < 0.01$  between groups. Data shown are representative of three independent replicates. h) Alcian blue staining was used to examine the effects of suramin on GAG expression in pellet culture of chondrocytes. Scale bar = 50  $\mu$ m. i) Immunofluorescence and immunohistochemistry for COL2A1 and COL1A1 on chondrocyte pellets in the presence or absence of 10  $\mu$ M suramin for 28 days.

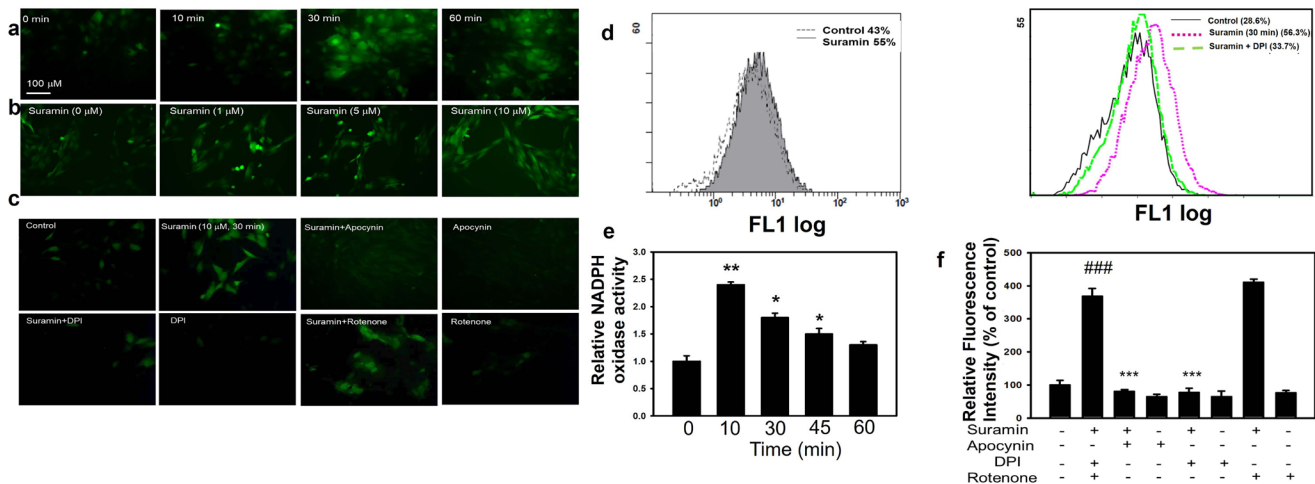


Fig. 2

Involvement of nicotinamide adenine dinucleotide phosphate (NADPH) oxidase (NOX) in the suramin-induced reactive oxygen species (ROS) production. Cells were treated with 0 to 10  $\mu\text{M}$  suramin for various time periods as indicated. Then, the cells were further incubated with 100  $\mu\text{M}$  dichloro-dihydro-fluorescein diacetate (DCFH-DA) for 30 minutes before detection of the fluorescence by fluorescence microscopy (magnification: 100 $\times$ ) (a, b, left panel) or by flow cytometry (d, left panel). c) Cells were pretreated with N-acetyl-L-cysteine (NAC) (c), rotenone (c), and diphenyleneiodonium chloride (DPI) (c, d) or vehicle, followed by treatment with 10  $\mu\text{M}$  suramin for 30 minutes. Then, the cells were further incubated with 100  $\mu\text{M}$  DCFH-DA for 30 minutes before detection of the fluorescence by fluorescence microscopy or by flow cytometry (a to d, f). Results are expressed as mean values; ### $p < 0.001$  compared to vehicle control and \*\*\* $p < 0.001$ , \*\* $p < 0.01$ , \* $p < 0.05$  compared to suramin treatment alone. e) Cells were treated with 10  $\mu\text{M}$  suramin for various time periods as indicated to measure their NOX activity, as described in the Methods section. f) Bar diagram showing quantitative data of 2',7'-dichlorofluorescein-positive cells.

Suramin is a highly sulphonated compound that is also known as a historic drug for the treatment of African sleeping sickness. Suramin has been reported to have several pharmacological effects, including anticancer, hepatoprotective, antioxidative, and relieving pathological pain.<sup>15,17–19</sup> It was also reported that suramin attenuated cartilage destruction in a rat model of rheumatoid arthritis by inhibiting proinflammatory cytokine production and protecting against cartilage damage in a papain-induced mouse model.<sup>13,14</sup> The chondroprotective effect appears to be mediated by a functional increase in tissue inhibitor of metalloproteinase 3 (TIMP-3) and a subsequent decrease in the activity of catabolic enzymes.<sup>19</sup> Our recent study demonstrated that suramin suppressed IL-1 $\beta$ -induced apoptosis, and down-regulated MMP-3, MMP-13, a disintegrin and metalloproteinase with thrombospondin motifs 4 (ADAMTS-4), and ADAMTS-5, while upregulating COL2A1 and ACAN in IL-1 $\beta$ -treated disc nucleus pulposus (NP) cells.<sup>20</sup> The morphological changes in chondrocytes during dedifferentiation resemble those occurring in OA chondrocytes, where chondrocytes undergo hypertrophic terminal differentiation, which features chondrocyte hypertrophic change, and eventually apoptosis. Our findings indicate that suramin may also be a potential agent for improving chondrogenic properties for the phenotypic maintenance of chondrocytes during *in vitro* expansion.

Articular cartilage lesions undergo self-healing with great difficulty, owing to their avascular nature and aneural structural organization. Several surgical techniques such as microfracture, osteochondral transplantation (OCT), ACI, and matrix-associated autologous

chondrocyte implantation (MACI) procedures have been demonstrated to be at least partially effective treatments of cartilage injury.<sup>21</sup> Until now, ACs have been the cell source for cartilage repair. Problematically, due to serial culture, AC dedifferentiation takes place, which may result in fibrocartilaginous tissue formation. In this study, we investigated the effect of suramin on ACs in cartilage cell therapies by detecting chondrogenic properties, including the expression of cartilage-related genes such as ACAN, SOX9, COL2A1, and COL1A1. In addition, we investigated redox signals that have been implicated in the regulation of suramin's ability to promote the maintenance phenotype of chondrocytes.

## Methods

**Porcine chondrocyte isolation.** All animal procedures were reviewed and approved by the Institutional Animal Care and Use Committee of Kaohsiung Medical University. Primary ACs were harvested from the articular cartilage (AC) of the femoral condyles of skeletally mature (6 to 8 m) male pigs. The harvested AC blocks were digested with 1.5 mg/ml collagenase type II in Dulbecco's Modified Eagle Medium-F12 (DMEM-F12) containing 10% foetal calf serum (FCS) at 37°C. Isolated chondrocytes were expanded using DMEM-F12 medium supplemented with 50 units/ml of penicillin, 50  $\mu\text{g}/\text{ml}$  of streptomycin, and 10% FBS. An ARRIVE checklist is included in the Supplementary Material to show that the ARRIVE guidelines were adhered to in this study.

**Western blot.** We followed the standard instructions.<sup>22</sup> The following primary antibodies were used: COL2A1 primary antibodies (1:1,000), ACA (1:1,000), COL10A1

(Abcam, UK) (1:1,000), NOX1 (1:1,000), NOX2 (1:1,000), NOX4 (1:1,000) (all ProteinTech Group, USA), p67<sup>phox</sup> (1:1,000) (Abclonal), phospho-extracellular signal-regulated kinase 1/2 (p-ERK1/2) (1:1,000; Cell Signaling Technology, USA), p-p38 (1:1,000; MyBioSource, USA), p-JNK (1:1,000; MyBioSource), ERK1/2 (1:1,000; Cell Signaling Technology), JNK (1:1,000; MyBioSource), and p38 (1:1,000; MyBioSource). The secondary antibody (1:5,000) was anti-rabbit peroxidase-conjugated (Jackson ImmunoResearch Europe, UK) and the chemiluminescence substrate was ECL Advance (GE Healthcare, USA). Abundance was quantified using Image-Pro Plus 6.0 software (Media Cybernetics, USA). Protease and phosphatase inhibitors were purchased from BIOTOOLS (Taiwan).

**RNA isolation and real-time PCR.** Total RNA was extracted using the RNAzol or TOOLS<sup>Smart</sup> RNA Extractor reagent (BIOTOOLS). Purified total RNA (2 µg) was reverse-transcribed using the Thermo Scientific Maxima First Strand cDNA Synthesis Kit (Thermo Fisher Scientific, USA) or TOOL SQuant (BIOTOOLS, Taiwan) according to the manufacturer's instructions. SYBR quantitative polymerase chain reaction (qPCR) was performed using the SYBR Green qPCR Mix (BIOTOOLS) kit and was processed on a LightCycler PCR and detection system (Roche Diagnostics, USA). Each reaction (20 µl) was run in duplicate and contained 1 µl of complementary DNA (cDNA) template along with the following primer sequences: *Col2a1*, forward (ACTCCTGGCACGGATGGTC) and reverse (CTTTCTACCAACATCGCCC); *Acan*, forward (CCCAACCAGCCTGACAACCTT) and reverse (CCTTCTCGTGCCAGATCATCA); *Col10a1*, forward (TGAAGTGGTTCATGGAGTGTTTTA) and reverse (TGCCTTGGTGTGGATGGT); *Col1a*, forward (CTGGTACG GCGAGAGCATGACC) and reverse (GGAGGAGCAGGG CCTTCTTGAG); and *glyceraldehyde 3-phosphate dehydrogenase (Gapdh)*, forward (TCACGACCATGGAGAAGGCT) and reverse (CAGGAGGCATTGCTGATGATC). Cycling parameters were 95°C for 15 minutes to activate DNA polymerase, followed by 40 cycles of 95°C for 15 seconds, 60°C for 20 seconds, and 72°C for 30 seconds. Melting curves were generated at the end of the reaction. Threshold cycles ( $C_t$ ) for each gene tested were normalized to the housekeeping GAPDH gene value ( $\Delta C_t$ ), and every experimental sample was referred to as the control ( $\Delta\Delta C_t$ ). Fold change values were expressed as  $2^{-\Delta\Delta C_t}$  values.

**Reverse transcriptase polymerase chain reaction.** Reverse transcriptase polymerase chain reaction (RT-PCR) was performed according to the manufacturer's instructions with a slight modification. The mixture contained 3 µg total RNA, 2.5 µM oligo(dT), 1.5 mM magnesium chloride (MgCl<sub>2</sub>), 0.01 M dithiothreitol, and 200 units of SuperScript III reverse transcriptase in a total volume of 20 µl. The RT steps consisted of a RT step (42°C for 60 minutes) and a denaturation step (70°C for five minutes). The PCR steps consisted of a denaturation step (95°C for 30 seconds), a primer annealing step (60°C for

30 seconds), and an elongation step (72°C for 30 seconds) for 30 cycles. In the final step, the duration of the elongation step was seven minutes. Finally, the samples were loaded onto a 1% agarose gel. The gels were then observed and photographed under ultraviolet light. The primers used were as follows: *Nox1*, sense primer 5'-CCATTCATATTCGACGAGCAGG-3' and antisense primer 5'-AACATCCTCACTGACAGTGCC-3'; *Nox2*, sense primer 5'-TTGGCGATCTCAGCAGAAGG-3' and antisense primer 5'-GAGGTCAGGGTCAAAGGGTG-3'; *Nox4*, sense primer 5'-TGGAACGCACTACCAGGATGTC-3' and antisense primer 5'-TGGAACGCACTACCAGGATGTC-3'; *p47*, sense primer 5'-CCTGTCTGAGAAGCTGGTCTACC-3' and antisense primer 5'-GCGCGCTGCAGTATTACTG-3'; *p67*, sense primer 5'-GAAGTCTGAGCCGAGACATTCC-3' and antisense primer 5'-AGCCCCGAGAAGCTGTCTTGATC-3'; and *Gapdh*, sense primer 5'-TCACGACCATGGAGAAGGCT-3' and antisense primer 5'-CAGGAGGCATTGCTGATGATC-3'. *Gapdh* messenger RNA (mRNA) expression was used as an internal control.

**Pellet cultures and chondrocyte redifferentiation.** To perform pellet culture, a method described by Kato et al<sup>23</sup> was used. Briefly, pellet cultures were prepared by adding  $1 \times 10^6$  cells in 15 ml conical polypropylene (PE) centrifuge tubes. The cells were pelleted by centrifugation at 400× g for five minutes at room temperature. The pellets were maintained in chondrogenic differentiation medium (DMEM-F12 supplemented with 10% FBS, 2% insulin-transferrin-selenium-ethanolamine, and 1% penicillin/streptomycin) without (control) or with the addition of 10 µM suramin. The pellets were cultured for four weeks, and were then collected for subsequent histological and immunofluorescence staining.

**Total glycosaminoglycans quantification.** Total sulphated glycosaminoglycan (GAG) content was determined in cell pellet by using 1,9-dimethylmethylene blue (DMMB; Polysciences). Chondroitin sulphate C from shark cartilage was used as a standard. Briefly, harvested pellets were digested at 56°C overnight with 0.1 M proteinase K in PBE buffer (100 mM Na<sub>2</sub>HPO<sub>4</sub>; 1 mM ethylenediaminetetraacetic acid (EDTA), pH 7.5; 10 mM Tris, pH 6.5), and 100 µl of the digested sample was combined with 1 ml dimethylmethylene blue dye solution, and the absorbance was measured at 656 nm. DNA was measured using Hoechst 33,258 dye (Thermo Fisher Scientific). Briefly, 10 µl of the digested sample was combined with 200 µl Hoechst dye solution (0.7 µg/ml). Fluorescence measurements were taken with an excitation wavelength of 340 nm and emission wavelength of 465 nm. A standard curve was generated using calf thymus DNA. The GAG content was normalized against the amount of DNA measured in each sample.

**Immunohistochemistry.** Pellet sections were fixed in 4% paraformaldehyde (ten minutes, room temperature (RT)) and washed in phosphate-buffered saline (PBS). Then, 5 µm thick sections were stained with 1% (w/v) Alcian blue 8 GX, in addition, and after blocking endogenous tissue peroxidase activity with 0.3% H<sub>2</sub>O<sub>2</sub> (ten minutes,

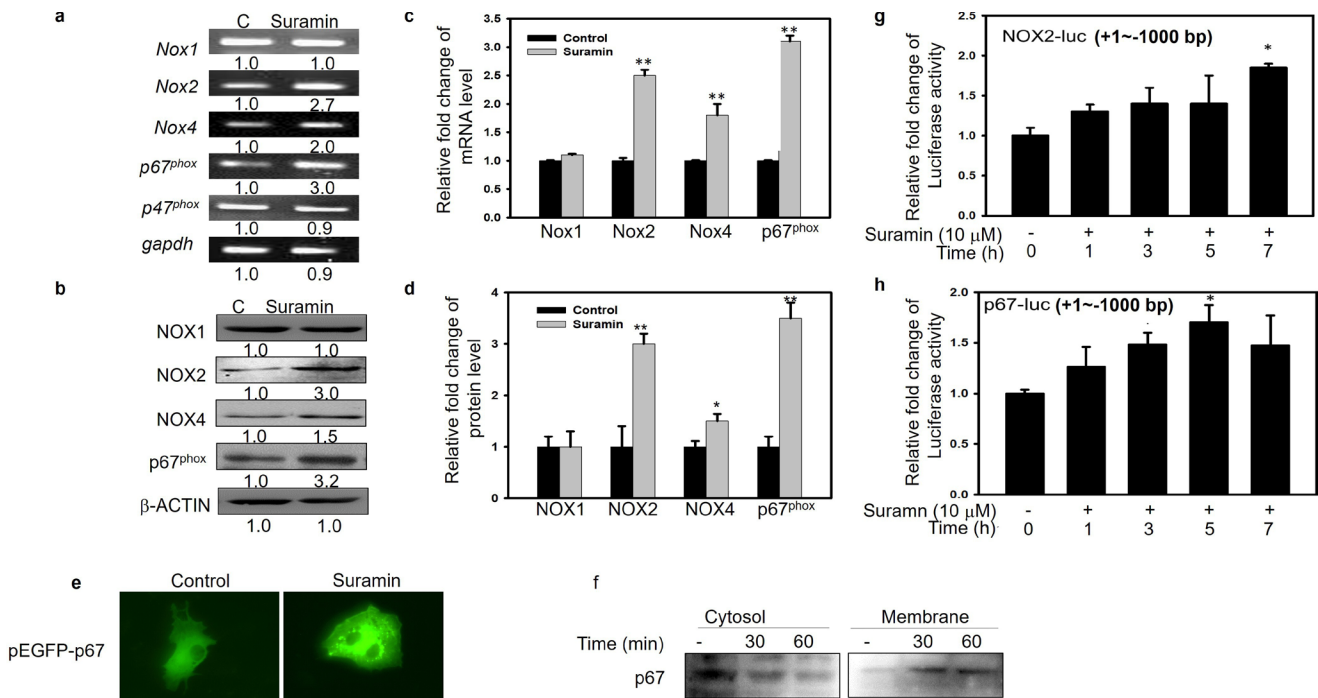


Fig. 3

Differential expression of nicotinamide adenine dinucleotide phosphate (NADPH) oxidase (NOX) during suramin-induced differentiation of primary chondrocytes. a) and c) The chondrocytes were treated with 10 μM suramin for 16 hours. Then we measured Nox1, Nox2, Nox4, p47, p67, and glyceraldehyde 3-phosphate dehydrogenase (Gapdh) messenger RNA (mRNA) levels using reverse transcriptase polymerase chain reaction (RT-PCR) and quantitative RT-PCR (qRT-PCR). b) and d) Total cell lysates were analyzed by western blot with specific antibodies as indicated. e) pEGFP-p67 plasmid was transiently transfected into chondrocytes and incubated with or without 10 mM of suramin. Thereafter, the cells were fixed with formaldehyde and permeabilized with Triton X-100. The images were observed with an immunofluorescence microscope through a 40× objective. f) Cells were treated with 10 μM suramin for 30 and 60 minutes. The cytoplasmic and membrane protein fractionations were collected as described in the Methods section to detect p67<sup>phox</sup> expression by western blot. g) and h) The chondrocytes were transfected with NOX2 or p67<sup>phox</sup> luciferase plasmid, respectively, and then incubated with 10 μM suramin for different times as indicated. The luciferase activity was determined and normalized with the amount of total protein. Values are means and standard deviations of triplicate measurements. \*p < 0.05, \*\*p < 0.01 compared with untreated control. C, control.

RT). Pellet sections were incubated with monoclonal mouse antibodies (mABs) against collagen type I diluted in 1:100 or collagen type II (1:100) (16 to 18 hours, 4°C). Then pellet sections were washed in washing buffer and incubated with a biotinylated horse-antirabbit immunoglobulin G (IgG) (Vector Laboratories, USA) (30 minutes, RT). Afterwards pellet sections were incubated with avidin-biotin-peroxidase complex (ABC; Abcam, USA). After repeated washing, the 3,3'-diaminobenzidine tetrahydrochloride (DAB) (Vector Laboratories) was added continuously for approximately four minutes without light. The reaction was stopped with aqua dest, and then the sections were counterstained with haematoxylin. Representative images were obtained using a microscope (NIKON Ti-U; EINST Technology, Singapore).

**ROS detection.** Non-fluorescent 2',7'-dichlorodihydrofluorescein diacetate (DCFH-DA) can be oxidized by ROS to highly fluorescent 2',7'-dichlorofluorescein (DCF). The chondrocytes were pretreated with 10 μM apocynin, 50 μM rotenone, 10 μM diphenyleneiodonium chloride (DPI), or vehicle combined with or without 10 μM suramin. The cells were then incubated with 100 μM DCFH-DA in DMEM for 30 minutes at 37°C and washed with ice-cold PBS to quantify the fluorescence emitted from the fluorescent DCF

using a fluorescence-activated cell sorter (FACScan; Becton Dickinson, USA), or by detection of the fluorescence by fluorescence microscopy at 488 nm excitation and 525 nm emission. Finally, photographs were taken using a fluorescence microscope equipped with a digital camera (NIKON Ti-U). For quantitative analysis of the fluorescence intensity, six image fields from each treatment were randomly selected, and the relative fluorescence intensity was measured using Image-Pro Plus 6.0.

**Determination of NOX activity.** Cells ( $2 \times 10^5$ ) were trypsinized and harvested by centrifugation at 400× g for ten minutes at 4°C and resuspended in ice-cold DMEM after treatment. The cells ( $2 \times 10^4$ ) were then added to prewarmed (37°C) DMEM containing 1 μM NADPH and 20 μM lucigenin to a final 600 μl volume to initiate the reaction, followed by immediate measurement of chemiluminescence using a chemiluminescence analyzer. Chemiluminescence was measured continuously at one-minute intervals for 15 minutes. The activity of NOX is expressed as counts per million cells.

**DNA constructs, transient transfection, and reporter gene assay.** The full-length cDNAs of porcine p67<sup>phox</sup> genes were amplified by PCR. The PCR products were digested with EcoRI/XbaI to generate fragments that were

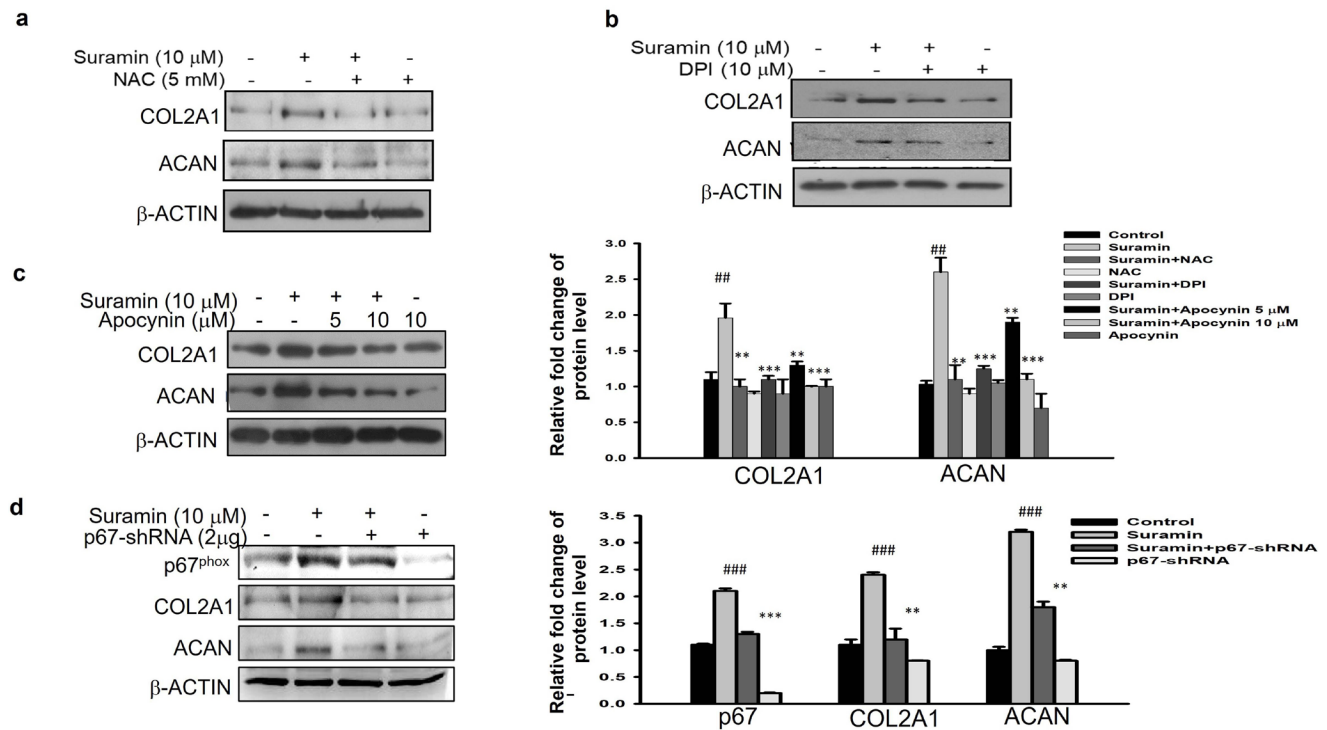


Fig. 4

Suramin positively regulated NOX2/p67<sup>phox</sup> expression and was involved in differentiation of primary chondrocytes. a) to c) The chondrocytes were pretreated with a) N-acetyl-L-cysteine (NAC), b) diphenyleneiodonium chloride (DPI), and c) apocynin for one hour followed by treatment with or without 10  $\mu$ M suramin for 24 hours. Total cell lysates were analyzed by western blot with specific antibodies as indicated. d) Chondrocytes were transfected with pLKO.1-p67<sup>phox</sup>-shRNA or empty vector followed by treatment with 10  $\mu$ M suramin for 24 hours, then total cell lysates were collected and subjected to western blot with specific antibodies as indicated. \*\* $p < 0.01$ , \*\*\* $p < 0.001$  compared with untreated control; ### $p < 0.001$  compared to the control. ACAN, aggrecan; COL2A1, collagen, type II, alpha 1; DPI, diphenyleneiodonium chloride; NOX, nicotinamide adenine dinucleotide phosphate (NADPH) oxidase; shRNA, short hairpin (sh) RNA.

then ligated into the pcDNA3.1/myc-His expression vector containing the cytomegalovirus (CMV) promoter and validated by sequencing. The porcine NOX2 and p67<sup>phox</sup> promoters from -1,000 to +1 bp were cloned by PCR using specific primers (p67<sup>phox</sup> sense: 5-AGA TCT GAG ATC CCT GTG TGC-3, antisense: 5-CCA TGG TCT TTT TAA AAA TTA TTT TTC C-3; NOX2 sense: 5-AGA TCT TGT TGG GTG TGA TTT TGA AT-3, antisense: 5-CCA TGG AGAAATTAGCAAATCATT-3) with porcine genomic DNA from porcine chondrocytes as a template. PCR products were cloned into the T&A cloning vector (Yeastern Biotech) and then confirmed by DNA sequencing. After digestion with BglIII and NcoI, the fragments were subcloned into the pGL3-basic vector (Promega, USA). The primers used to construct the  $\Delta$ AD (amino acid (a.a) 199 to 212),  $\Delta$ AD (a.a 199 to 212), sense: 5' GCCAAGAAGGAT TACAGCTTCTCGGGCTTTGCC 3', antisense: 5'GGGG CAAAGCCCGAGAAGCTGTAATCCTTCTTGGC 3'). Site-directed mutagenesis was performed using the Agilent QuikChange site-directed mutagenesis kit (Agilent Technologies, USA) and confirmed by sequencing. The pLKO.1-p67-short hairpin (sh) RNA (shRNA), which targets the porcine p67 gene sequence 5-GCCAAGAA GGAGGAATGGAAA-3, and luciferase control (pLKO.1-shLuc) plasmid constructs were kindly obtained from

the National RNAi Core Facility located at the Institute of Molecular Biology/Genomic Research Centre, Academia Sinica (Taiwan), supported by the National Research Programme for Genomic Medicine Grants of the National Science Council (NSC97-3112-B-001-016). Transfection was performed using Lipofectamine 2000 reagent according to the manufacturer's instructions with slight modifications. Chondrocytes were subcultured in a 12-well plate for 24 hours before transfection at a density of  $8 \times 10^4$  cells in 0.5 ml of fresh culture medium per well. For use in the transfection assay, plasmids were mixed with Lipofectamine 2000 reagent in Opti-MEM (Thermo Fisher Scientific) and incubated at room temperature for 20 minutes. Cells were incubated in the mixture for a further 48 hours, and then lysed to measure luciferase activity as described previously.<sup>24</sup> Luciferase activity was measured and normalized to the amount of total protein. **Immunofluorescence analysis.** Chondrocytes were transfected with pEGFP-p67 expression plasmid or incubated with or without 10  $\mu$ M suramin for 24 hours and then plated on glass coverslips. The cells were washed and fixed with 4% paraformaldehyde for 20 minutes at room temperature, permeabilized with 0.2% Triton X-100, and then blocked with 10% FBS in PBS. The cells were then stained with anti-COL2A1 (1:200) (Proteintech Group)

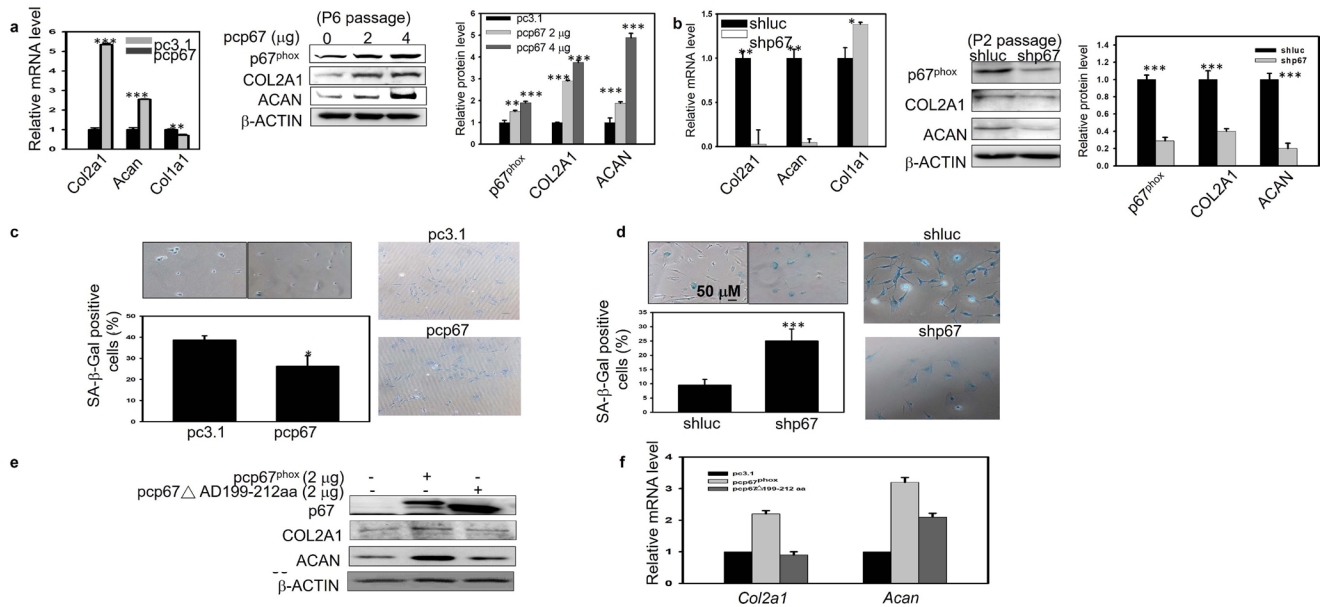


Fig. 5

Differentiation of primary chondrocytes in depleted and overexpressed  $p67^{phox}$ . a) Later passage of chondrocytes were transiently transfected with various doses of  $p67^{phox}$  (pcDNA-  $p67^{phox}$ ) or control (pcDNA3.1) plasmid for additional 24 hours, to detect the messenger RNA (mRNA) and protein expression of chondrogenic and differentiation marker as indicated by using reverse transcriptase polymerase chain reaction (RT-PCR) or western blot. b) Early stage of chondrocytes were transfected with specific shRNA of  $p67^{phox}$  (pLKO.1- $p67^{phox}$ -shRNA) or a luciferase control (pLKO.1-shLuc) to measure mRNA and protein expression of chondrogenic and differentiation marker as indicated by using RT-PCR or western blot. The expression of *glyceraldehyde 3-phosphate dehydrogenase* (*Gapdh*) or  $\beta$ -ACTIN was used as an internal control of RT-PCR or western blot, respectively. c) Late passage of primary chondrocytes were treated as in Figure 5a, and senescence-associated  $\beta$ -galactosidase (SA- $\beta$ -gal) activity and Alcian Blue staining (left panel) were used to detect these. Representative photomicrograph of the SA- $\beta$ -gal assay is shown. The percentage of  $\beta$ -galactosidase-positive cells in each group was compared and is illustrated in the histogram;  $n = 3$  in each experiment. d) Early passage of chondrocyte were treated as in Figure 5b, and senescence-associated  $\beta$ -galactosidase (SA- $\beta$ -gal) activity and Alcian Blue staining (magnification: 100 $\times$ ) (left panel) were used to detect these. Representative photomicrograph of the SA- $\beta$ -gal assay is shown. The percentage of  $\beta$ -galactosidase-positive cells in each group was compared and is illustrated in the histogram;  $n = 3$  in each experiment. e) and f) The chondrocytes were transiently transfected with  $p67^{phox}$  (pcDNA- $p67^{phox}$ ),  $pcp67^{\Delta}$  AD (a.a 199 to 212), or control (pcDNA3.1) plasmid, to detect the mRNA and protein expression of COL2A1 and aggrecan as indicated by using RT-PCR or western blot. \* $p < 0.05$ , \*\* $p < 0.01$ , \*\*\* $p < 0.001$  compared with untreated control. shRNA, short hairpin (sh) RNA.

and COL10A1 (Abcam) (1:200) antibody. Images were captured using a fluorescence microscope (NIKON Ti-U). **Stable  $p67^{phox}$ -silencing early passage (P2) chondrocyte transfectants.** A total of 293 T cells ( $8 \times 10^6$ ) were incubated in 10 cm petri dishes coated with poly-L-lysine for 24 hours to package lentiviral vectors. TransIT-LT1 reagent (45  $\mu$ l) in Opti-MEM (750  $\mu$ l) was mixed with the packaging vector pCMV- $\Delta$ R8.91 (6.75  $\mu$ g), the envelope vector pMD.G (0.75  $\mu$ g), and the transfer vector pLKO.1- $p67$ -shRNA (7.5  $\mu$ g) or pLKO.1-shluc (7.5  $\mu$ g). After incubation at room temperature for 20 minutes, the plasmid-containing mixture was transferred to 293 T cells for 16 hours. After 1% (w/v) bovine serum albumin-containing medium was added for two days, the supernatant of the cultured cells was harvested. The media containing lentiviral vectors were centrifuged at 2,500 rpm for ten minutes, and the viral supernatants were passed through 0.45  $\mu$ m filters and stored at  $-80^{\circ}\text{C}$ . P3 chondrocytes ( $5 \times 10^5$ ) were cultured on 6 cm petri dishes with 4 ml medium, followed by infection with the harvested lentiviral supernatants (1 ml) and polybrene (8  $\mu$ g/ml) for 24 hours. The infected cells were incubated in 2  $\mu$ g/ml puromycin-containing

medium for selection of stable  $p67^{phox}$ -silencing primary chondrocyte transfectants.

**Statistical analysis.** Each result in this study is from at least three independent experiments. Significant differences were evaluated using the independent-samples *t*-test. All values are displayed as means and standard deviations (SDs) for three determinations ( $p < 0.05$ ;  $p < 0.01$ ;  $p < 0.001$  compared with vehicle). Statistical significance was set at  $p < 0.05$ .

## Results

**Chondrocytes expanded in a suramin-containing medium acquire enhanced redifferentiation capacity.** We assessed whether exposure to suramin preserved chondrogenic properties in ACs. As shown in Figures 1a and 1b, exposure of chondrocytes (P3 passage) to suramin resulted in a time- and dose-dependent increase in the protein expression of COL2A1 and ACAN. The expression of ACAN was rapidly elevated as early as one hour and continuously for at least one week (data not shown), and the protein expression of COL2A1 was also increased at eight hours and was sustained for up to one week (data not shown) after suramin administration. In

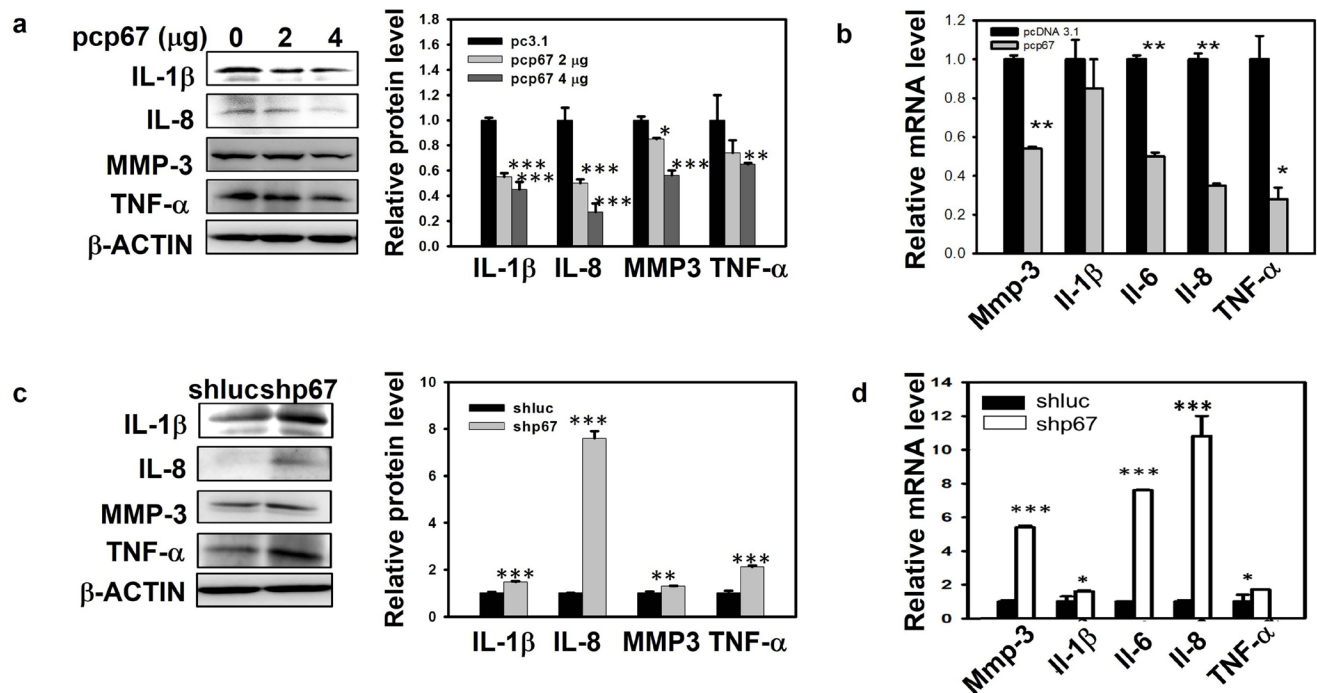


Fig. 6

Effect on dedifferentiation marker expression in depleted and overexpressed p67<sup>phox</sup>. a) and b) The chondrocytes were transiently transfected with various doses of p67<sup>phox</sup> plasmid (pcDNA-p67<sup>phox</sup>) or control (pcDNA3.1) to detect messenger RNA (mRNA) and protein expression of dedifferentiation marker as indicated by using reverse transcriptase polymerase chain reaction (RT-PCR) or western blot. c) and d) The chondrocytes were transfected with specific shRNA of p67<sup>phox</sup> (pLKO.1-p67<sup>phox</sup>-shRNA) or a luciferase control (pLKO.1-shLuc) to measure mRNA and protein expression of dedifferentiation marker as indicated by using RT-PCR or western blot. The expression of *glyceraldehyde 3-phosphate dehydrogenase (gapdh)* or β-actin was used as an internal control of RT-PCR or western blot, respectively. Results are expressed as mean value; \*\*\*p < 0.001, \*\*p < 0.01, \*p < 0.05 compared to transfected with the pcDNA or shLuc plasmid. IL, interleukin; MMP, matrix metalloproteinase; shRNA, short hairpin (sh) RNA; TNF, tumour necrosis factor.

contrast, the protein expression of COL10A1 decreased in a dose-dependent manner after chondrocyte treatment. Using real-time PCR, *Col2a1* and *Acan* transcripts were transiently increased by suramin at eight and 16 hours, to evaluate the redifferentiation capacity of expanded chondrocytes. The earlier and later passages of chondrocytes from P1 and P6 were used, and chondrogenic (COL2A1 and ACAN) and dedifferentiation (COL1A and COL10A1) markers were investigated. As shown in Figures 1d to 1f, the mRNA and protein levels of COL2A1 and ACAN were dramatically reduced from passages P1 to P6. Despite a sharp decrease in COL2A1 and ACAN expression levels in chondrocytes from passages P1 to P6, the mRNA and protein expression levels of COL2A1 and ACAN were significantly higher when P1 and P6 chondrocytes were incubated with suramin for seven days. Regarding the dedifferentiation marker, the mRNA levels of *Col1a* and *Col10a1* were detected in the passaged chondrocytes. In the earlier passage (P1), the expression of *Col1a* and *Col10a1* was significantly lower in the chondrocytes than in the later passage (P6). However, the mRNA expression levels of *Col1a1* and *Col10a1* were perceptibly reduced when P1 and P6 chondrocytes were coincubated with suramin at day 7. Furthermore, the ratios of COL2/COL1, which represent the degree of dedifferentiation, were also quantified.<sup>25</sup>

High values of these ratios revealed an advantageous status of differentiation (of native healthy cartilage), whereas low values indicated dedifferentiated cells.<sup>26</sup> As shown in Figure 1f, the ratios of COL2/COL1 were clearly increased in suramin administration of chondrocytes, regardless of the earlier passage (P1) or later passage cells (P6). To confirm the above data, immunofluorescence was used to detect the expression of COL2A1 and COL10A1 on day 7. As shown in Figure 1g, expanded chondrocytes from P1 and P6 yielded a higher chondrogenic index (COL2A1), whereas the chondrocytes from P1 and P6 exhibited a lower dedifferentiation index (COL10A1) after a seven-day incubation with suramin. Further, to investigate the chondrogenic potential of suramin on redifferentiation of expanded chondrocytes, we performed 3D pellet culture using P3 chondrocytes, and the pellets were cultured with or without the supplement of the suramin in chondropermissive medium for 28 days. Glycosaminoglycan (GAG) and collagen production were evaluated by quantitative biochemical analyses (DMMB assay), Alcian blue staining, as well as immunohistochemistry. The results were as shown in Figures 1g and 1h; after 28 days of subsequent 3D pellet culture, GAG and proteoglycan production was significantly higher in pellets of chondrocytes that were expanded in the presence of suramin

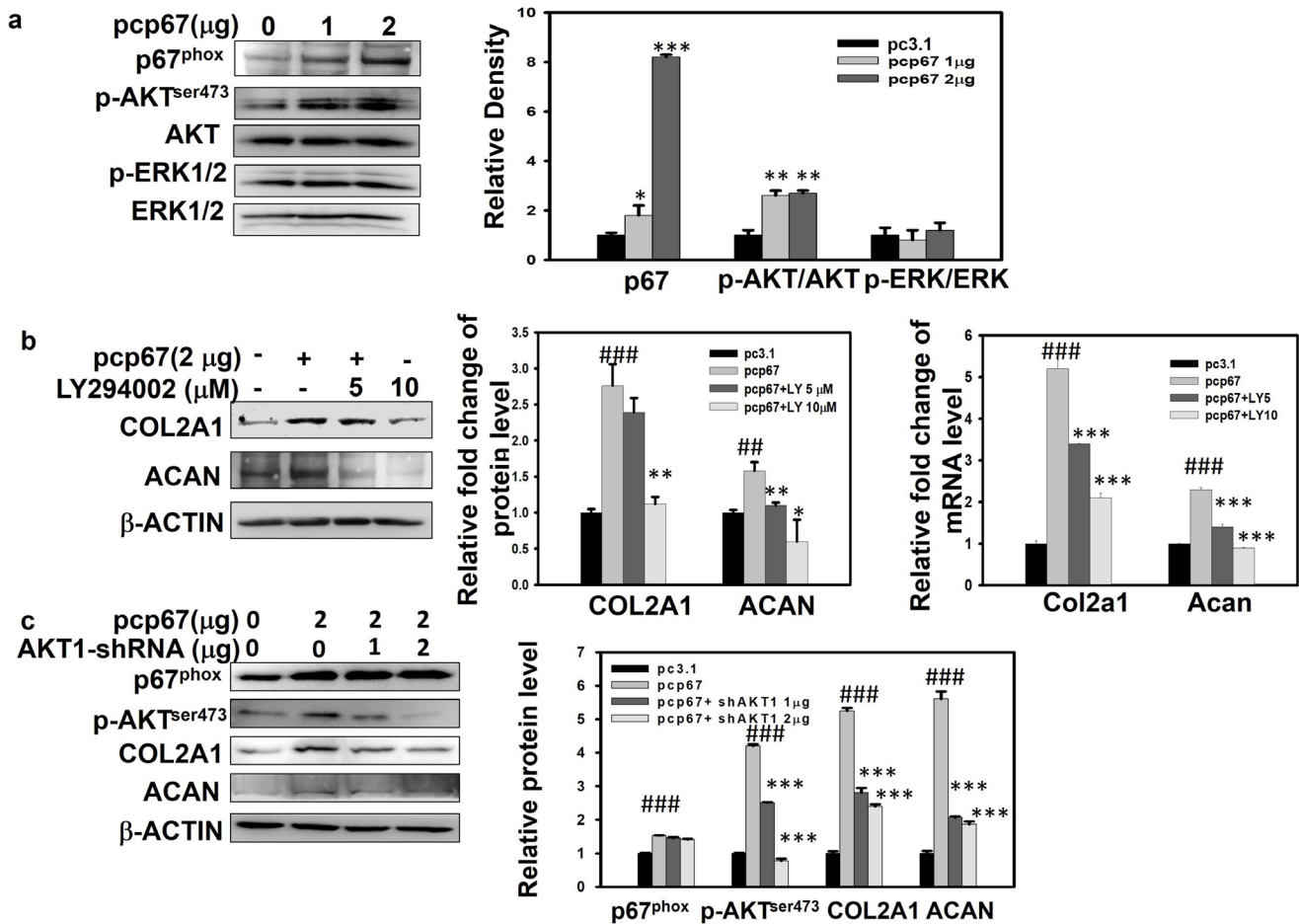


Fig. 7

Phosphoinositide 3-kinase/protein kinase B (PI3K/AKT) pathway was involved in p67<sup>phox</sup>-induced chondrocyte differentiation. a) The relationship between the ERK and PI3K/AKT pathway and p67<sup>phox</sup> was also measured in chondrocytes by western blot analysis.  $\beta$ -actin served as protein loading control. \* $p < 0.05$ , \*\* $p < 0.01$ , \*\*\* $p < 0.001$  compared to transfected pcDNA alone. b) Later passage of chondrocytes were transiently transfected with various doses of p67<sup>phox</sup> plasmid (pcDNA-p67<sup>phox</sup>) or control (pcDNA3.1). p67<sup>phox</sup>-overexpressed cells were pretreated with either 5 or 10  $\mu$ mol/l of LY294002 for three hours, and then the expression of collagen, type II, alpha 1 (COL2A1) and aggrecan (ACAN) protein was measured by western blot analysis. Each assay was performed in triplicate, and the results shown as means (standard deviations (SDs)) of four independent experiments ( $p < 0.001$ ). c) The pcp67<sup>phox</sup> plasmids (1  $\mu$ g) were used to cotransfect chondrocytes with pLKO.1-AKT1-shRNA (1 or 2  $\mu$ g) for 24 hours, and the cell lysates were harvested to determine p67, p-AKT<sup>ser473</sup>, COL2A1, ACAN, and  $\beta$ -ACTIN expression. ### $p < 0.001$ , ## $p < 0.01$  compared to transfected pcDNA alone; \* $p < 0.05$ , \*\* $p < 0.01$ , \*\*\* $p < 0.001$  compared to transfected with wild type of pcp67 plasmid. shRNA, short hairpin (sh) RNA.

compared to controls as shown by the DMMB assay and Alcian blue staining. Additionally, pellets cultured under supplementation with suramin (10  $\mu$ M) also revealed a stronger staining for COL2A1 when compared to the control group. Conversely, immunofluorescence staining and immunohistochemistry revealed a slight decrease in COL1A1 production in suramin administration pellets (Figure 1i). Collectively, these results indicate that chondrocytes expanded in the presence of suramin maintain their redifferentiation potential.

**Suramin-induced superoxide generation originates from NADPH oxidase.** Many studies have demonstrated that the redox status of chondrocytes plays an essential role in the regulation of chondrocyte differentiation and chondrogenesis.<sup>13,16,27</sup> ROS are also suggested to be potential mediators of suramin-regulated signalling.<sup>28,29</sup> Further elucidation of their roles in suramin enhanced

the redifferentiation capacity and induced signalling. Using DCFH-DA as an indicator, cells were stimulated with different doses of suramin for various time periods and their ROS production was detected by fluorescence microscopy and flow cytometry, respectively. The results showed that suramin induced a rapid increase in ROS production up to 10 mins after stimulation (Figure 2a). We found that suramin-induced ROS generation in a time- and dose-dependent manner (Figures 2a and 2b) and ROS production were significantly suppressed by the NOX inhibitor DPI, an NADPH oxidase inhibitor, and apocynin (Figures 2d and 2f),<sup>30</sup> but not by allopurinol (xanthine oxidase inhibitor) and rotenone (mitochondrial complex I inhibitor) (data not shown). Therefore, we hypothesized that the major source of O<sub>2</sub><sup>-</sup> production in response to suramin might be NOX. As shown in Figure 2e, the NOX oxidase activity was induced by

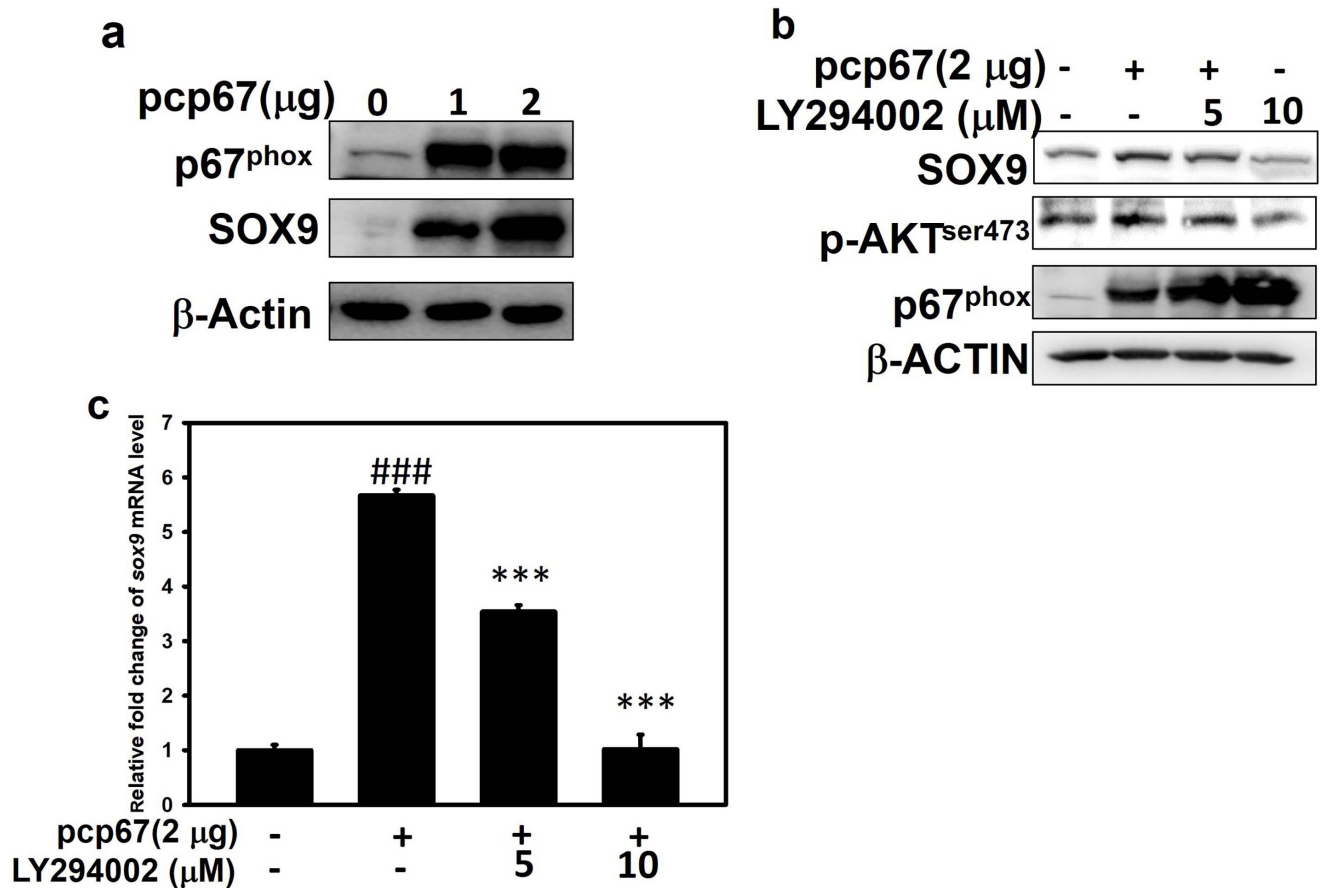


Fig. 8

p67<sup>phox</sup>-induced chondrocyte differentiation was dependent on PI3K/AKT/SOX9 pathways. a) The chondrocytes were transiently transfected with various doses of p67<sup>phox</sup> plasmid (pcDNA-p67<sup>phox</sup>) or control (pcDNA3.1), and then the expression of p67<sup>phox</sup> and SOX9 protein was measured by western blot analysis. b) and c) The chondrocytes were transiently transfected with various doses of p67<sup>phox</sup> plasmid (pcDNA-p67<sup>phox</sup>) or control (pcDNA3.1). p67<sup>phox</sup>-overexpressed cells were pretreated with either 5 or 10 μmol/l of LY294002 for three hours, and then the protein and messenger RNA (mRNA) expression of SOX9 was measured by western blot and real-time reverse transcriptase-polymerase chain reaction (RT-PCR) analysis. ###p < 0.001 compared with transfected pcDNA alone; \*\*\*p < 0.001 compared with untreated control. AKT, protein kinase B; PI3K, phosphoinositide 3-kinase; SOX9, SRY-box transcription factor 9.

suramin to a peak at ten minutes and was sustained for at least one hour.

**Superoxide mediates suramin-induced differentiation of chondrocytes.** To determine which members of the NOX family might be responsible for suramin-induced ROS generation in chondrocytes, we examined the abundance of various NOX family members by RT-PCR and western blot analysis. The genes for *Nox1*, *Nox2*, and *Nox4*, as well as those for the cytosolic components *p47phox* and *p67phox* were expressed in chondrocytes (Figure 3a). In contrast, *Nox3* and *Nox5* were not detected at all (data not shown). The mRNA and protein levels of NOX2, NOX4, and *p67phox* were increased after the suramin incubation of chondrocytes (Figures 3a and 3b). These changes in *Nox1*, *Nox2*, and *Nox4* gene expression were confirmed by real-time qPCR analysis (Figure 3c). To determine whether suramin controls the transcriptional activity of NOX2 and p67, a reporter containing 1.0 kb of the porcine NOX2 and p67<sup>phox</sup> promoter (-1,000 to +1 bp) fused with the firefly luciferase gene was constructed, as

described in the Methods section. Then, we transiently transfected the reporter into chondrocytes and measured its promoter activity in response to suramin. As shown in Figures 3g and 3h, suramin induced NOX2 and p67<sup>phox</sup> promoter activity by approximately twofold in chondrocytes. Furthermore, chondrocytes were transiently transfected with expression vectors for wild-type p67<sup>phox</sup> tagged at its carboxy terminus with the green fluorescent protein epitope and plated onto coverslips. Immunofluorescence analysis of unstimulated cells revealed a pattern of staining indicative of a cytosolic distribution of ectopically expressed p67<sup>phox</sup>. No nuclear staining was evident, whereas only minor staining was observed on the periphery of the cell. Stimulation of cells with suramin produced a marked alteration in the cellular distribution of p67<sup>phox</sup> with a sharply defined edge to the cells, indicative of plasma membrane localization (Figure 3e). As expected, after treatment with suramin for 30 minutes, cytoplasmic p67<sup>phox</sup> is translocated from the cytosol to the membrane fraction (Figure 3f), which is consistent with the activation of

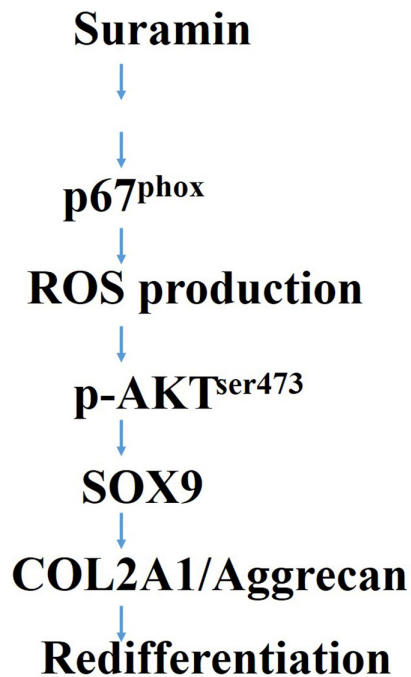


Fig. 9

Scheme illustrating the possible mechanism of suramin-regulated cellular differentiation of chondrocytes. AKT, protein kinase B; COL2A1, collagen, type II, alpha 1; ROS, reactive oxygen species; SOX9, SRY-box transcription factor 9.

NOX (Figure 2e). In addition, the enhanced effect of suramin on the expression of NOX2/p67<sup>phox</sup> was more obvious than that of NOX4. Therefore, we suggest that the major source of suramin-induced ROS production in chondrocytes might be NOX2/p67<sup>phox</sup> complex activation. As described above, suramin was shown to promote chondrocyte differentiation (Figure 1). Moreover, the role of O<sub>2</sub><sup>-</sup> in suramin-induced chondrocyte redifferentiation was explored. As shown in Figures 4a to 4d, western blot analysis revealed that suramin increased the protein expression of COL2A1 and ACAN, which are major chondrogenic marker genes. Pretreatment with NAC, DPI, and apocynin blocked suramin-induced O<sub>2</sub><sup>-</sup> production (Figures 2d and 2e), and inhibited suramin-induced increase in COL2A1 and ACAN expression (Figures 4a to 4c). Knockdown of the p67<sup>phox</sup> subunit by shRNA blocked the suramin-induced protein expression of COL2A1 and ACAN (Figure 4d). Together, these results suggest that suramin-induced ROS production generated by NOX2/p67<sup>phox</sup> activation is required for the cellular differentiation of chondrocytes.

**p67<sup>phox</sup> are required for differentiation in primary chondrocytes.** The role of p67<sup>phox</sup> in chondrocyte phenotype maintenance was further confirmed by determining the gene expression of chondrogenic differentiation markers in p67<sup>phox</sup>-depleted early passage (more differentiated) primary chondrocytes or overexpression of p67<sup>phox</sup> in late passage chondrocytes (less differentiated cells). Overexpression of p67<sup>phox</sup> in late passage chondrocytes (P6) markedly enhanced the protein and

mRNA expression of COL2A1 and ACAN (Figure 5a). Furthermore, the senescence rate was significantly decreased (Figure 5c, left panel), and the production of proteoglycan stained by Alcian blue was significantly enhanced (Figure 5c, right panel). Conversely, knockdown of p67<sup>phox</sup> by its specific shRNA (pLKO.1-p67<sup>phox</sup>-shRNA) (shp67<sup>phox</sup>) in early passage chondrocytes (P2) suppressed the protein and mRNA expression of COL2A1 and ACAN (Figures 5b and 5d), proteoglycan production, and senescence percentage. Further, to investigate whether p67-mediated ROS generation is required for regulated chondrocyte phenotype, we used a p67<sup>phox</sup> mutant, p67<sup>phox</sup> ( $\Delta$ AD), which cannot support ROS production,<sup>31</sup> and transiently transfected with these mutant plasmids into chondrocytes, as shown in Figures 5e and 5f. The mean increased protein and mRNA level of COL2A1 and ACAN was obviously lower than the cells that transfected with the wild type form of p67<sup>phox</sup> (pcp67<sup>phox</sup>) (COL2A1, wild type p67<sup>phox</sup> transfected vs p67<sup>phox</sup> ( $\Delta$ AD) : 2.1 (standard deviation (SD)) 0.1) vs 0.9 (SD 0.1); ACAN, wild type p67<sup>phox</sup> transfected vs p67<sup>phox</sup> ( $\Delta$ AD) : 3.2 (SD 0.15) vs 2.0 (SD 0.12)). In addition, overexpression of p67<sup>phox</sup> in chondrocytes (P6), the protein and mRNA levels of MMP-3, IL-1 $\beta$ , IL-6, IL-8, and tumour necrosis factor alpha (TNF $\alpha$ ), which are known regulators of dedifferentiation, were suppressed (Figures 6a and 6b); in contrast, knockdown of p67<sup>phox</sup> in chondrocytes (P2), the mRNA and protein expression of MMP-3, IL-1 $\beta$ , IL-6, IL-8, and TNF $\alpha$  were markedly upregulated (Figures 6c and 6d). These results indicate that p67<sup>phox</sup> potentiates chondrogenic differentiation in vitro.

**p67<sup>phox</sup>-dependent modulation of the chondrocyte phenotype is AKT-dependent.** Intracellular mitogen-activated protein kinases mitogen-activated protein kinases (MAPKs) and protein kinase B (AKT) are the major oxidative stress-sensitive signal transduction pathways that influence cell proliferation, survival, and differentiation.<sup>32</sup> In addition, phosphoinositide 3-kinase (PI3K)-AKT signalling is a key regulator of cell survival in response to growth factor stimulation and promotes proteoglycan synthesis, type II collagen synthesis, SOX9 expression, and chondrocyte survival.<sup>33</sup> We thus examined the phosphorylation of ERK1/2 and AKT. Immunoblot analysis revealed that phosphorylation of AKT and ERK1/2 was greatly increased in chondrocytes treated with suramin (data not shown), and the phosphorylation of AKT was obviously upregulated in cells overexpressing p67<sup>phox</sup> (Figure 7a). In contrast, phosphorylation of ERK in cells transfected with p67<sup>phox</sup> did not change compared with that in cells transfected with the control (Figure 7a). Therefore, we explored whether p67<sup>phox</sup>-induced differentiation effects were mediated through the PI3K/AKT pathway. Figures 7b and 7c, show that pretreatment with the PI3K inhibitor LY294002 could attenuate both suramin (data not shown) and p67<sup>phox</sup>-induced COL2A1 and ACAN expression in chondrocytes. Furthermore, knockdown of

AKT1 by its specific shRNA in chondrocytes could decrease suramin (data not shown) and p67<sup>phox</sup>-induced COL2A1 and ACAN expression. Therefore, we suggest that p67<sup>phox</sup> generates ROS-mediated suramin-induced differentiation of chondrocytes by regulating the PI3K/AKT pathway.

**p67<sup>phox</sup> mediates maintenance of articular chondrocyte phenotypic stability through AKT-dependent SOX9 expression.** We then investigated the question of which molecular mechanism links p67<sup>phox</sup>/PI3K/AKT signalling to the maintenance of phenotypic stability. It is known that SOX9 mediates anabolic signalling in human chondrocytes.<sup>34,35</sup> Therefore, we tested the hypothesis that p67<sup>phox</sup> signalling supports SOX9 expression via AKT activation. Hence, we transfected wild-type p67<sup>phox</sup> (pcp67) into primary chondrocytes and found increased expression of SOX9 (Figure 8a). Pretreatment with the PI3K-specific pharmacological inhibitor LY294002 blocked p67<sup>phox</sup>-induced mRNA and protein expression of SOX9. These results suggest that p67 activates the PI3K/AKT pathway to increase SOX9 expression, thereby promoting the phenotypic maintenance of chondrocytes.

## Discussion

ACI was first developed by Brittberg et al<sup>22</sup> in 1994 and has been reported as a promising strategy for the clinical treatment of full-thickness cartilage defects. However, the insufficient cell number and gradual loss of phenotype of chondrocytes when expanded in vitro diminished its clinical application. Therefore, new therapeutic drugs are required that enhance the therapeutic applications.

In this study, we introduced suramin, a drug developed long ago, and investigated its molecular effect on the phenotype maintenance of chondrocytes cultured in vitro. As described in other reports, suramin treatment increased GAGs in the chondrogenic cell line ATDC5 micromass model of chondrogenesis and in pellet cultures of human ACs.<sup>36</sup> In addition, suramin inhibits cartilage degradation in OA by increasing TIMP-3 levels.<sup>37</sup> Our novel findings have further proved that suramin can promote the gene expression of COL2A1 and ACAN while downregulating the gene expression of COL1A1 and COL10A1 in both early and late passage chondrocytes (Figure 1). We suggest that suramin could prevent or delay chondrocyte dedifferentiation.

Furthermore, we demonstrated that suramin-induced NOX activation to produce ROS contributes to the phenotype maintenance of chondrocytes. Several previous studies have shown that ROS is considered a pathogenic factor in OA by regulating intracellular signalling, chondrocyte senescence and apoptosis, and matrix-degrading protease synthesis.<sup>38-41</sup> For example, tert-butylhydroquinone (tBHQ) is a synthetic phenolic antioxidant that has potent antioxidant activities, and applying tBHQ demonstrated notably attenuated cartilage destruction in destabilization of the medial meniscus (DMM)-induced OA in vivo.<sup>42</sup> Conversely,

another study has demonstrated that wogonin induces mild generation of ROS, thereby regulating the cellular redox status causing the induction of NF-E2-related factor 2/antioxidant response element (Nrf2/ARE) pathways through activation of the ROS/ERK/Nrf2/HO-1-SOD2-NQO1-GCLC signalling axis in OA chondrocytes.<sup>43</sup> In our recent report, we found that shockwave treatment enhanced ECM synthesis in ACs through activation of the ROS/MAPK/NRF2 signalling pathway.<sup>44</sup> Furthermore, another study showed that increased stiffness and appropriate ROS production facilitates the chondrogenic differentiation of bone marrow-derived mesenchymal stem cells (BMSCs) by activating the mechanistic target of rapamycin (mTOR) signalling pathway.<sup>45</sup> Therefore, ROS are not categorically harmful, and therapeutics must consider the essential role of ROS levels.

In addition, we demonstrated that NOX2/p67<sup>phox</sup> activation is a major source of suramin-induced ROS production (Figure 3). Many studies have attested to the functional relationship between the NOX family and increased ROS generation in various cell types. For example, NOX4 is the main NOX enzyme involved in the early stages of haematopoietic differentiation from human-induced pluripotent stem cells.<sup>46</sup> NOX4 is overexpressed in pre-adipocytes and participates in the differentiation of stem cells into adipocytes.<sup>47</sup> Polyphyllin VII blocks the differentiation of bone marrow macrophages (BMMs) into osteoclasts by inhibiting ROS synthesis, which is regulated by the TRAF6-cSrc-PI3K signalling pathway, including Nox1 and Rac family small GTPase 1 (GTP-Rac1).<sup>48</sup> Superoxide generation by the NR2B-NMDARs/RasGRF1/NOX2 pathway promotes dendritogenesis.<sup>49</sup> We also proved that Nox2/p67<sup>phox</sup> is involved in suramin-induced chondrocyte redifferentiation. Collectively, these results indicate that the Nox family plays an important role in the phenotype maintenance of chondrocytes during in vitro culture expansion, and should be further examined. In the present study, suramin upregulated the promoter activation of NOX2 and p67<sup>phox</sup> (Figure 3). This indicates that suramin might regulate the biosynthesis of NOX2 and p67<sup>phox</sup> partially at the transcriptional level. However, compared with the fold change of Nox2 and p67<sup>phox</sup> mRNA after suramin treatment (Figures 3a and 3c; approximately 2.5- and 3-fold), this result highlighted that a mRNA stability regulation mechanism may be involved in the expression of NOX2 and p67<sup>phox</sup>. However, the molecular regulation should be further elucidated.

It is known that phosphate plays an important role in the regulation of chondrocyte proliferation and differentiation, as well as endochondral bone development. A previous study found that overexpression of mutated *solute carrier family 20 member 2 (SLC20A2)* gene enhances the expression of ACAN, COL2A1, and SOX9, and inhibits hypertrophic differentiation while decreasing inorganic phosphate (Pi) uptake in ATDC5 chondrocytes.<sup>50</sup> Suramin is also known as a

purinergic receptor (P2 receptor) inhibitor; in addition, purine receptors are important regulators of extracellular inorganic pyrophosphate (ePPi) production by chondrocytes. P1 receptor stimulation diminishes and P2 receptor stimulation enhances ePPi production, respectively. Hence, suramin decreases ePPi concentrations in porcine cartilage explants and chondrocyte monolayers.<sup>51</sup> However, whether suramin enhanced the phenotype maintenance via regulation of extracellular phosphate concentration needs to be further investigated.

In this study, overexpression of p67<sup>phox</sup> could enhance the protein production of SOX9, COL2A1, and ACAN in chondrocytes. Further, we performed the DNA affinity precipitation assay and chromatin-immunoprecipitation assay and found that SOX9 protein binding to the Col2a1 promoter was increased after suramin administration for 24 hours in chondrocytes or in p67-overexpressed chondrocytes (Supplementary Figure a, right panel), which demonstrated that the process of suramin mediating the gene expression of Col2a1 was at least partially dependent on transcriptional level. Differently, we added cycloheximide to block de novo protein synthesis in disc nucleus pulposus (NP) cells (data not shown), and the protein degradation rate of COL2A1 and ACAN was slower in suramin-treated group compared to control group (Supplementary Figure a, left panel). It is suggested that suramin regulated the COL2A1 and ACAN expression in disc NP cells at least partially through post-translational modification. In addition, in the present study the PI3K/AKT pathway mediated p67-induced SOX9, COL2A1, and ACAN production. The PI3K/AKT pathway has been implicated in chondrocyte proliferation and survival,<sup>52,53</sup> chondrogenic differentiation, hypertrophic maturation, and ECM deposition.<sup>54,55</sup> As shown in Figure 7, overexpression of p67<sup>phox</sup> in chondrocytes activated AKT phosphorylation. This also shows that ROS can stimulate AKT phosphorylation in phagocytic and nonphagocytic cells.<sup>56,57</sup> Another study reported that oxidative stress activates PI3K/AKT-dependent signalling via the inactivation of PTEN.<sup>58</sup> Therefore, elucidating the crosstalk between the PI3K/AKT pathway and NOX2/p67<sup>phox</sup> activation requires further investigation.

In conclusion, our study provides evidence that in chondrocytes, suramin-increased Nox2/p67<sup>phox</sup> expression can promote complex activation to produce ROS release. The increased oxidative stress might inhibit PTEN to further activate the PI3K/AKT pathway and stimulate the expression of SOX9/COL2A/ACAN to promote phenotype maintenance of chondrocytes (Figure 9). These novel findings highlight that suramin can be an effective therapeutic strategy for cartilage repair in ACL applications.

## Supplementary material



Figure showing the DNA affinity precipitation assay and chromatin-immunoprecipitation assay, and an ARRIVE checklist showing that the ARRIVE guidelines were adhered to in this study.

## References

- Candela ME, Yasuhara R, Iwamoto M, Enomoto-Iwamoto M. Resident mesenchymal progenitors of articular cartilage. *Matrix Biol.* 2014;39:44–49.
- Frisbie DD, Bowman SM, Colhoun HA, DiCarlo EF, Kawcak CE, McIlwraith CW. Evaluation of autologous chondrocyte transplantation via a collagen membrane in equine articular defects: results at 12 and 18 months. *Osteoarthritis Cartilage.* 2008;16(6):667–679.
- Charlier E, Deroyer C, Ciregia F, et al. Chondrocyte dedifferentiation and osteoarthritis (OA). *Biochem Pharmacol.* 2019;165:49–65.
- Benya PD, Padilla SR, Nimni ME. Independent regulation of collagen types by chondrocytes during the loss of differentiated function in culture. *Cell.* 1978;15(4):1313–1321.
- Kawakami Y, Rodriguez-León J, Izpisua Belmonte JC. The role of TGFbetas and Sox9 during limb chondrogenesis. *Curr Opin Cell Biol.* 2006;18(6):723–729.
- Benya PD, Shaffer JD. Dedifferentiated chondrocytes reexpress the differentiated collagen phenotype when cultured in agarose gels. *Cell.* 1982;30(1):215–224.
- Kolettas E, Buluwela L, Bayliss MT, Muir HI. Expression of cartilage-specific molecules is retained on long-term culture of human articular chondrocytes. *J Cell Sci.* 1995;108 ( Pt 5):1991–1999.
- Chen Z, Zhang Z, Guo L, et al. The role of histone deacetylase 4 during chondrocyte hypertrophy and endochondral bone development. *Bone Joint Res.* 2020;9(2):82–89.
- Yang J, Zhou Y, Liang X, Jing B, Zhao Z. MicroRNA-486 promotes a more catabolic phenotype in chondrocyte-like cells by targeting SIRT6: possible involvement in cartilage degradation in osteoarthritis. *Bone Joint Res.* 2021;10(7):459–466.
- Choudhary D, Adhikary S, Ahmad N, et al. Prevention of articular cartilage degeneration in a rat model of monosodium iodoacetate induced osteoarthritis by oral treatment with Withaferin A. *Biomed Pharmacother.* 2018;99:151–161.
- Henrotin YE, Bruckner P, Pujol J-P. The role of reactive oxygen species in homeostasis and degradation of cartilage. *Osteoarthritis Cartilage.* 2003;11(10):747–755.
- Funato S, Yasuhara R, Yoshimura K, et al. Extracellular matrix loss in chondrocytes after exposure to interleukin-1 $\beta$  in NADPH oxidase-dependent manner. *Cell Tissue Res.* 2017;368(1):135–144.
- Ambe K, Watanabe H, Takahashi S, Nakagawa T. Immunohistochemical localization of Nox1, Nox4 and Mn-SOD in mouse femur during endochondral ossification. *Tissue Cell.* 2014;46(6):433–438.
- Del Carlo M, Loeser RF. Nitric oxide-mediated chondrocyte cell death requires the generation of additional reactive oxygen species. *Arthritis Rheum.* 2002;46(2):394–403.
- Cheng G, Cao Z, Xu X, van Meir EG, Lambeth JD. Homologs of gp91phox: cloning and tissue expression of Nox3, Nox4, and Nox5. *Gene.* 2001;269(1–2):131–140.
- Kim KS, Choi HW, Yoon HE, Kim IY. Reactive oxygen species generated by NADPH oxidase 2 and 4 are required for chondrogenic differentiation. *J Biol Chem.* 2010;285(51):40294–40302.
- Grange L, Nguyen MVC, Lardy B, et al. NAD(P)H oxidase activity of Nox4 in chondrocytes is both inducible and involved in collagenase expression. *Antioxid Redox Signal.* 2006;8(9–10):1485–1496.
- Yoshimura K, Miyamoto Y, Yasuhara R, et al. Monocarboxylate transporter-1 is required for cell death in mouse chondrocytic ATDC5 cells exposed to interleukin-1 $\beta$  via late phase activation of nuclear factor kappaB and expression of phagocyte-type NADPH oxidase. *J Biol Chem.* 2011;286(17):14744–14752.
- McGeary RP, Bennett AJ, Tran QB, Cosgrove KL, Ross BP. Suramin: clinical uses and structure-activity relationships. *Mini Rev Med Chem.* 2008;8(13):1384–1394.
- Liu Z-M, Lu C-C, Shen P-C, et al. Suramin attenuates intervertebral disc degeneration by inhibiting NF- $\kappa$ B signalling pathway. *Bone Joint Res.* 2021;10(8):498–513.
- Binder H, Hoffman L, Zak L, Tiefenboeck T, Aldrian S, Albrecht C. Clinical evaluation after matrix-associated autologous chondrocyte transplantation: a comparison of four different graft types. *Bone Joint Res.* 2021;10(7):370–379.
- Brittberg M, Lindahl A, Nilsson A, Ohlsson C, Isaksson O, Peterson L. Treatment of deep cartilage defects in the knee with autologous chondrocyte transplantation. *N Engl J Med.* 1994;331(14):889–895.

23. Kato Y, Iwamoto M, Koike T, Suzuki F, Takano Y. Terminal differentiation and calcification in rabbit chondrocyte cultures grown in centrifuge tubes: regulation by transforming growth factor beta and serum factors. *Proc Natl Acad Sci U S A*. 1988;85(24):9552–9556.
24. Liu ZM, Tseng HY, Tsai HW, Su FC, Huang HS. Transforming growth factor  $\beta$ -interacting factor-induced malignant progression of hepatocellular carcinoma cells depends on superoxide production from Nox4. *Free Radic Biol Med*. 2015;84:54–64.
25. Marlovits S, Hombauer M, Truppe M, Vécsei V, Schlegel W. Changes in the ratio of type-I and type-II collagen expression during monolayer culture of human chondrocytes. *J Bone Joint Surg Br*. 2004;86-B(2):286–295.
26. Martin I, Jakob M, Schäfer D, Dick W, Spagnoli G, Heberer M. Quantitative analysis of gene expression in human articular cartilage from normal and osteoarthritic joints. *Osteoarthritis Cartilage*. 2001;9(2):112–118.
27. Morita K, Miyamoto T, Fujita N, et al. Reactive oxygen species induce chondrocyte hypertrophy in endochondral ossification. *J Exp Med*. 2007;204(7):1613–1623.
28. Sauer H, Klimm B, Hescheler J, Wartenberg M. Activation of p90RSK and growth stimulation of multicellular tumor spheroids are dependent on reactive oxygen species generated after purinergic receptor stimulation by ATP. *FASEB J*. 2001;15(13):2539–2541.
29. Sciancalepore M, Luin E, Parato G, et al. Reactive oxygen species contribute to the promotion of the ATP-mediated proliferation of mouse skeletal myoblasts. *Free Radic Biol Med*. 2012;53(7):1392–1398.
30. Heumüller S, Wind S, Barbosa-Sicard E, et al. Apocynin is not an inhibitor of vascular NADPH oxidases but an antioxidant. *Hypertension*. 2008;51(2):211–217.
31. Han CH, Freeman JL, Lee T, Motalebi SA, Lambeth JD. Regulation of the neutrophil respiratory burst oxidase. Identification of an activation domain in p67(phox). *J Biol Chem*. 1998;273(27):16663–16668.
32. Matsuzawa A, Ichijo H. Stress-responsive protein kinases in redox-regulated apoptosis signaling. *Antioxid Redox Signal*. 2005;7(3–4):472–481.
33. Yin W, Park JI, Loeser RF. Oxidative stress inhibits insulin-like growth factor-I induction of chondrocyte proteoglycan synthesis through differential regulation of phosphatidylinositol 3-Kinase-Akt and MEK-ERK MAPK signaling pathways. *J Biol Chem*. 2009;284(46):31972–31981.
34. Bi W, Deng JM, Zhang Z, Behringer RR, de Crombrughe B. Sox9 is required for cartilage formation. *Nat Genet*. 1999;22(1):85–89.
35. Han Y, Lefebvre V. L-Sox5 and Sox6 drive expression of the aggrecan gene in cartilage by securing binding of Sox9 to a far-upstream enhancer. *Mol Cell Biol*. 2008;28(16):4999–5013.
36. Guns L-A, Monteagudo S, Kvasnytsia M, et al. Suramin increases cartilage proteoglycan accumulation in vitro and protects against joint damage triggered by papain injection in mouse knees in vivo. *RMD Open*. 2017;3(2):e000604.
37. Chanalaris A, Doherty C, Marsden BD, et al. Suramin inhibits osteoarthritic cartilage degradation by increasing extracellular levels of chondroprotective tissue inhibitor of metalloproteinases 3. *Mol Pharmacol*. 2017;92(4):459–468.
38. Yu SM, Kim SJ. Withaferin A-caused production of intracellular reactive oxygen species modulates apoptosis via PI3K/Akt and JNKinase in rabbit articular chondrocytes. *J Korean Med Sci*. 2014;29(8):1042–1053.
39. Rao Z, Wang S, Wang J. Peroxiredoxin 4 inhibits IL-1 $\beta$ -induced chondrocyte apoptosis via PI3K/AKT signaling. *Biomed Pharmacother*. 2017;90:414–420.
40. Yu SM, Kim SJ. The thymoquinone-induced production of reactive oxygen species promotes dedifferentiation through the ERK pathway and inflammation through the p38 and PI3K pathways in rabbit articular chondrocytes. *Int J Mol Med*. 2015;35(2):325–332.
41. Zuo D, Tan B, Jia G, Wu D, Yu L, Jia L. A treatment combined prussian blue nanoparticles with low-intensity pulsed ultrasound alleviates cartilage damage in knee osteoarthritis by initiating PI3K/Akt/mTOR pathway. *Am J Transl Res*. 2021;13(5):3987–4006.
42. Zhang H, Li J, Xiang X, et al. Tert-butylhydroquinone attenuates osteoarthritis by protecting chondrocytes and inhibiting macrophage polarization. *Bone Joint Res*. 2021;10(11):704–713.
43. Khan NM, Haseeb A, Ansari MY, Devarapalli P, Haynie S, Haqqi TM. Wogonin, a plant derived small molecule, exerts potent anti-inflammatory and chondroprotective effects through the activation of ROS/ERK/Nrf2 signaling pathways in human osteoarthritic chondrocytes. *Free Radic Biol Med*. 2017;106:288–301.
44. Shen P-C, Chou S-H, Lu C-C, et al. Shockwave Treatment Enhanced Extracellular Matrix Production in Articular Chondrocytes Through Activation of the ROS/MAPK/Nrf2 Signaling Pathway. *Cartilage*. 2021;13(2\_suppl):238S–253S.
45. Zheng L, Liu S, Cheng X, et al. Intensified stiffness and photodynamic provocation in a collagen-based composite hydrogel drive chondrogenesis. *Adv Sci (Weinh)*. 2019;6(16):1900099.
46. Brault J, Vigne B, Meunier M, et al. NOX4 is the main NADPH oxidase involved in the early stages of hematopoietic differentiation from human induced pluripotent stem cells. *Free Radic Biol Med*. 2020;146:107–118.
47. Schröder K, Wandzioch K, Helmcke I, Brandes RP. Nox4 acts as a switch between differentiation and proliferation in preadipocytes. *Arterioscler Thromb Vasc Biol*. 2009;29(2):239–245.
48. Zhou L, Song H, Zhang Y, Ren Z, Li M, Fu Q. Polyphyllin VII attenuated RANKL-induced osteoclast differentiation via inhibiting of TRAF6/c-Src/PI3K pathway and ROS production. *BMC Musculoskelet Disord*. 2020;21(1):112.
49. Abarzúa S, Ampuero E, van Zundert B. Superoxide generation via the NR2B-NMDAR/RasGRF1/NOX2 pathway promotes dendritogenesis. *J Cell Physiol*. 2019;234(12):22985–22995.
50. Li Y, Lin X, Zhu M, et al. A mutation in *SLC20A2* (c.C1849T) promotes proliferation while inhibiting hypertrophic differentiation in ATDC5 chondrocytes. *Bone Joint Res*. 2020;9(11):751–760.
51. Rosenthal AK, Hempel D, Kurup IV, Masuda I, Ryan LM. Purine receptors modulate chondrocyte extracellular inorganic pyrophosphate production. *Osteoarthr Cartil*. 2010;18(11):1496–1501.
52. Liu Q, He F, Zhou P, et al. HMGB2 promotes chondrocyte proliferation under negative pressure through the phosphorylation of AKT. *Biochim Biophys Acta Mol Cell Res*. 2021;1868(11):119115.
53. Huang L-W, Huang T-C, Hu Y-C, et al. S-Equal protects chondrocytes against sodium nitroprusside-caused matrix loss and apoptosis through activating PI<sub>3</sub>K/Akt pathway. *Int J Mol Sci*. 2021;22(13):7054.
54. Harrington EK, Coon DJ, Kern MF, Svoboda KKH. PTH stimulated growth and decreased Col-X deposition are phosphatidylinositol-3,4,5 triphosphate kinase and mitogen activating protein kinase dependent in avian sterna. *Anat Rec (Hoboken)*. 2010;293(2):225–234.
55. Hubchak SC, Sparks EE, Hayashida T, Schnaper HW. Rac1 promotes TGF-beta-stimulated mesangial cell type I collagen expression through a PI3K/Akt-dependent mechanism. *Am J Physiol Renal Physiol*. 2009;297(5):F1316–23.
56. Yen C-C, Hsiao C-D, Chen W-M, et al. Cytotoxic effects of 15d-PGJ2 against osteosarcoma through ROS-mediated AKT and cell cycle inhibition. *Oncotarget*. 2014;5(3):716–725.
57. Yu SM, Kim SJ. Thymoquinone-induced reactive oxygen species causes apoptosis of chondrocytes via PI3K/Akt and p38kinase pathway. *Exp Biol Med (Maywood)*. 2013;238(7):811–820.
58. Kwon J, Lee S-R, Yang K-S, et al. Reversible oxidation and inactivation of the tumor suppressor PTEN in cells stimulated with peptide growth factors. *Proc Natl Acad Sci U S A*. 2004;101(47):16419–16424.

#### Author information:

- Z-M. Liu, PhD, Assistant Researcher
- P-C. Shen, MD, Orthopaedic Assistant Professor
- S-H. Chou, MD, Orthopaedic Surgeon  
Department of Orthopedics, Kaohsiung Medical University Hospital, Kaohsiung Medical University, Kaohsiung, Taiwan.
- C-C. Lu, MD, Orthopaedic Associate Professor, Department of Orthopedics, Kaohsiung Medical University Hospital, Kaohsiung Medical University, Kaohsiung, Taiwan; Department of Orthopedics, Faculty of Medical School, College of Medicine, Kaohsiung Medical University, Kaohsiung, Taiwan; Department of Orthopaedic Surgery, Kaohsiung Municipal Siaogang Hospital, Kaohsiung, Taiwan; Regenerative Medicine and Cell Therapy Research Center, Kaohsiung Medical University, Kaohsiung, Taiwan.
- Y-C. Tien, MD, PhD, Orthopaedic Professor, Department of Orthopedics, Kaohsiung Medical University Hospital, Kaohsiung Medical University, Kaohsiung, Taiwan; Department of Orthopedics, Faculty of Medical School, College of Medicine, Kaohsiung Medical University, Kaohsiung, Taiwan.

#### Author contributions:

- Z-M. Liu: Conceptualization, Data curation, Methodology, Writing – original draft.
- P-C. Shen: Conceptualization, Data curation, Methodology, Writing – original draft.
- C-C. Lu: Investigation.
- S-H. Chou: Investigation.
- Y-C. Tien: Conceptualization, Data curation, Formal Analysis, Investigation, Methodology, Writing – review & editing.

- Z-M. Liu and P-C. Shen are joint first authors.

#### Funding statement:

- The authors disclose receipt of the following financial or material support for the research, authorship, and/or publication of this article: financial support by a grant from the Ministry of Science and Technology (Taipei, Taiwan; MOST 108-2314-B-037 -060 - and 110-2314-B-037 -030 - ) and Kaohsiung Medical University Chung-Ho Memorial Hospital (grant number: 103-3M35, 110-0R53, and 107-7M27).

#### ICMJE COI statement:

- All authors declare no conflicts of interest.

**Acknowledgements:**

- We appreciate the support from members of the Orthopedic Department of Kaohsiung Medical University Chung-Ho Memorial Hospital and the College of Medicine of Kaohsiung Medical University, Kaohsiung, Taiwan.

**Ethical review statement:**

- This study was approved by the Institutional Animal Care and Use Committee (IACUC) of Kaohsiung Medical University (KMU-108122).

**Open access funding**

- The authors report that they received open access funding for their manuscript from the Ministry of Science and Technology.

© **2022 Author(s) et al.** This is an open-access article distributed under the terms of the Creative Commons Attribution Non-Commercial No Derivatives (CC BY-NC-ND 4.0) licence, which permits the copying and redistribution of the work only, and provided the original author and source are credited. See <https://creativecommons.org/licenses/by-nc-nd/4.0/>